RSC Advances

ROYAL SOCIETY OF CHEMISTRY

www.rsc.org/advances

Journal Name

RSCPublishing

ARTICLE

Enhancement of the non-thermal plasma-catalytic system with different zeolites for toluene removal

Cite this: DOI: 10.1039/x0xx00000x

www.rsc.org/

Rong Huang,[a,c] Meijuan Lu,[a] Peitao Wang [a], Yangda Chen [a], Junliang Wu [a,b],Mingli Fu [a,b],Limin Chen [a,b] and Daiqi Ye[a,b,*]

Based on the important effect of catalyst on the plasma-catalytic system, various types of zeolites (5A, HZSM-5, Hβ, HY and Ag/HY) were chosen as catalysts to remove toluene under non-thermal plasma condition in this work. The results showed that all the zeolites, whether with toluene adsorption ability or not, significantly enhanced the toluene removal efficiency in the plasma discharge zone. Moreover, the carbon balance and CO_2 selectivity showed the same tendency of Ag/HY >HY > Hβ (HZSM-5)>5A, which was basically consistent with toluene adsorption ability, while opposed with the ozone emission. Loading silver on zeolite greatly decreased organic byproducts emission, and further improved the mineralization of toluene oxidation. At the same time, the intermediates including ring-opening products on the catalyst surface were identified, and the pathways of toluene decomposition were proposed.

1. Introduction

Volatile organic compounds (VOCs) have received increasing attention in recent years because of their harmfulness to human health and environment. They are regarded as precursor of photochemical smog and dust-haze[1]. Although relevant laws and regulations have been legislated in many countries to reduce VOCs emission, the terminal treatment technologies were still indispensable for VOCs reduction in most countries, especially in developing countries. Some conventional treatment technologies including liquid absorption, active carbon adsorption, thermal incineration and thermal catalytic oxidation were widely used and played important roles in VOCs removal, however, each of these technologies has its practical limitations[2-4]. Thus, new technologies have been researched and developed, among which plasma-catalysis technology shows the promising performance for VOCs removal because it combined the advantages of high selectivity from catalysis and rapid reaction from non-thermal plasma (NTP) at room temperature and atmospheric pressure[5].

In recent years the technology of non thermal plasma combined with catalysts in VOCs degradation has been extensively investigated and developed [6-8].In this technology, catalysts play important roles in the improvement of VOCs removal. One side, catalysts can prolong the gas retention time and increase the concentration of VOCs in the discharge zone, leading to higher collision probability between VOCs molecules and active species [3, 9].Research showed that the excellent adsorption ability of catalysts could improve the VOCs removal in the plasma[10, 11]. Moreover, adsorption ability was closely related with pore structure of catalyst. When the pore diameter of the catalyst was bigger than the VOC molecule diameter, the VOC could be adsorbed and enter into internal pore of catalyst. Conversely, when the by-product molecular was greater than the pore diameter, the phenomena of carbon deposition would appear. It was agreed that various catalysts have different pore diameters, so the pore diameter has very important effect both on adsorption ability of catalysts and carbon deposition of byproducts. On the other side, in the plasma system, the microdischarge might be generated inside the catalyst pores,

resulting in more discharge per unit volume and new reactive species formed in the pores of catalysts. These reactive species may promote VOCs decomposition[12]. Therefore, it was necessary to study the influence of pore size of catalysts on the removal and mineralization of VOCs by NTP combined with catalysts.

As traditional adsorbents, zeolites had unique micropores, cavies and channels in their frame structures. The size of their micropores range from 3 to 20 Å and it is comparable to the dynamic diameters of some molecules[13]. The shape selectivity of zeolites can enable selective removal of certain gas molecules, and meanwhile zeolites can easily interact with discharge plasma due to a very strong natural electric field within their framework[14]. Increasing studies focused on combining plasma with zeolites, and this system has been used for the removal of benzene[9], toluene[15, 16], xylene[17], and methane conversion[18, 19].These studies paid great attention to VOC removal or conversion by certain zeolite combined in the NTP system, while the relationship between pore sizes of zeolite and the performance of plasma-catalytic oxidation of VOCs is unclear currently.

In this work, toluene (molecule diameter is 5.89 Å)[20] , which is widely used in many fields of industry, was chosen as a target VOC. And a series of zeolites including 5A, HZSM-5, Hβ and HY were used as catalysts and their pore diameters were 5 Å, 5.5Å, 6.6 Å and 7.4 Å, respectively. Because silver-based materials are an outstanding catalysts in many catalytic oxidation reactions, such as oxidation of CO, benzyle alcohol and styrene[21], silver loaded zeolite HY was also studied. With these zeolites combined in NTP reaction, the toluene removal efficiency, carbon balance and CO_2 selectivity were evaluated, and the possible mechanism of toluene oxidation in NTP-catalytic system was present based on the analysis of byproducts in this study and those in literature.

2. Experimental

2.1. Experimental setup

The experimental setup is illustrated in Fig.1 and it consists of dielectric barrier discharge (DBD) plasma reactor, reaction gas supply system, and analytical instrumentation. The reactor was a quartz glass tube with an inner diameter of 10 mm and wall thickness of 1 mm. A stainless steel cylinder (i.d.2 mm) was used as the ground electrode, while a piece of stainless steel mesh (38 mm× 18 mm) covered around the outside surface of the quartz tube as the high voltage electrode. The effective discharge length and discharge gap were 18 mm and 4 mm, respectively. The reactor was energized by an AC high voltage power supply with the frequency of 2 kHz (CTP-2000k, Corona Laboratory, Nanjing, China). The discharge power was measured by an oscilloscope (TDS1002, Tektronix) and the typical power in the catalyst-plasma reactor was in the range of 3.3-3.7 W.For the plasma driven catalysis process, zeolite catalysts were partly placed in the discharge zone.

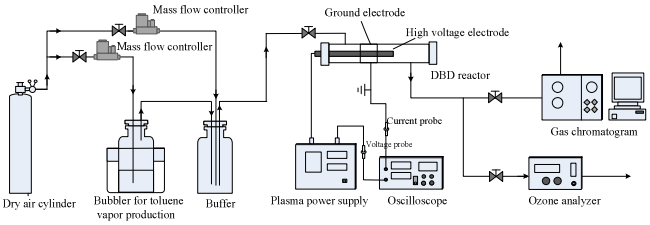

Fig. 1 Schematics of the experimental set up

Experiments were carried out at room temperature and atmospheric pressure. Gas toluene was introduced with dry air as carrier gas flow through pure liquid toluene kept in an ice and water bath. The air flow rate was adjusted by mass flow controllers. The reaction gas containing 100 ppm toluene passed through the discharge zone and catalyst bed at a rate of 300 ml/min, and the gas residence time in the catalyst bed was 0.15 s. When the toluene adsorption reached saturation, the plasma reaction was started, and meanwhile started to record the concentration of toluene, CO and CO_2 in the outlet gas. Toluene removal efficiency (TRE), carbon balance and CO_2 selectivity (CO_2%) were defined as follows:

$$TRE(\%) = \frac{[toluene]_{inlet} - [toluene]_{ontlet}}{[toluene]_{inlet}} \times 100\% \quad (1)$$

$$\text{Carbon balance}(\%) = \frac{[CO] + [CO_2]}{7([toluene]_{inlet} - [toluene]_{ontlet})} \times 100\% \quad (2)$$

$$CO_2 \text{ selectivity}(\%) = \frac{[CO_2]}{7([toluene]_{inlet} - [toluene]_{ontlet})} \times 100\% \quad (3)$$

2.2. Analytical method

Toluene concentration was analyzed on line using a gas chromatograph (GC-2014C, Shimadzu), equipped with two FID detectors. One detector is for organic compounds detection with a 30 m TG-WAXMS capillary column (30 m, 0.32 mm), the other, equipped with a methanizer, is for carbon monoxide and carbon dioxide analysis with a 5A molecular sieve (2 m, 2 mm) and Poraplot Q column (4 m, 2 mm). The concentration of ozone was monitored by an ozone analyzer (IDEAL-1000, IDEAL instrument).

Organic byproducts on the catalysts surface were extracted by CS_2 solution (Chromatographic Grade), and then were filtered with an ultrafiltration membrane to get liquid samples which were qualitatively analyzed by a gas chromatograph/mass spectrometry (GCMS-QP2010,Shimadzu) with an Rtx-5MS capillary column. The initial column temperature was 40℃, maintained for 2 min, and then increased to 220□ at the rate of 6□/min and maintained for 5 min. MS identification was conducted by NIST 08 databank (NIST/EPA/NIH Mass Spectra Library)

2.3. Catalysts preparation and characterization

Zeolites（5A, HZSM-5, Hβ and HY）were provided by Nan Kai University catalysts, Co. China. Their basic parameters were listed in Table1. The zeolites were powders as received, and before use they were compressed into flakes using a hydraulic press, followed by crushing and sieving into particles with the size of 40-60 mesh. The particle size range was selected to limit the pressure drop across the catalyst bed.

Silver supported zeolite catalysts were prepared by impregnation method as follows:.0.1575g $AgNO_3$ was dissolved in 60 ml of ethanol at room temperature, and then 2 g of zeolite powder was added into the above solution with stirring. The mixture was covered with PE film, stirred at room temperature for 16 h, and then put into a 60□ water bath to undergo the solvent evaporation, followed by calcinations in air at 500□ for 4 h in a muffle furnace. The resulting catalyst powder was converted to particles with the size of 40-60 mesh by the same method as stated above before use. The theoretical loading amount of silver deduced from chemical analysis was 5 wt%.

Table 1 Composition and pore diameters of the zeolites used

Type	FWT[a]	Pore diameter(Å)	Si/Al
5A	LTA	5	2
HZSM-5	MFI	5.5	25
Hβ	BEA	6.6	25
HY	FAU	7.4	5.3

[a] Framework Type

To study the effect of the zeolite structure on the catalytic activity, some characterization including X-ray patterns (XRD), scanning electron microscope (SEM) and XPS were measured. XRD patterns were collected by the Bruker D8 diffracometer operated at 30 kV and 30 mA using Cu Kα radiation. Scans were recorded in the range of 2θ between 20 and 80° with a scanning rate of 0.03 s^{-1}.SEM microphotographs were obtained with an electron microscope operating at 5.0 kV(S-3700N, Hitachi, Japan). The valences of Ag on the catalyst surface were analyzed by Kratos AXIS Ultra DLD spectrometer (Shimadzu, Japan).

3. Results and discussion

3.1. Toluene adsorption on various types of zeolites

Adsorption of toluene was carried out in a fixed adsorption bed. The breakthrough curves (Fig.2) were obtained at room temperature with a gas hourly space velocity (GHSV) of about 24,000 h^{-1}. The result showed that only zeolite 5A did not adsorb toluene, and other zeolites displayed different toluene adsorption ability with an order of HY >Hβ>HZSM-5.This result was well correlated to the framework structure of zeolites. The pore diameter of zeolite 5A is less than the mean aerodynamic diameter of toluene molecule. However, zeolites of HY, Hβ and HZSM-5 all have a relatively large 12-ring channel, and the dimensions are 7.4 Å×7.4 Å ,6.6 Å ×6.7 Å and 6.9 Å×6.9 Å ,respectively[22], which are somewhat larger than the molecular size of toluene. Therefore zeolites HY，Hβ and HZSM-5 could provide enough internal surface to adsorb toluene molecule, while zeolite 5A could not. It was also observed that zeolite HY had better toluene adsorption capacity than HZSM-5 and Hβ, may be due to its surface acidic characteristics resulted from lower Si/Al ratio than that of HZSM-5 and Hβ[23]. Compared to HY, the toluene adsorption greatly improved when the silver was loaded on it, and Ag/HY showed the best toluene adsorption capability among all the catalysts.

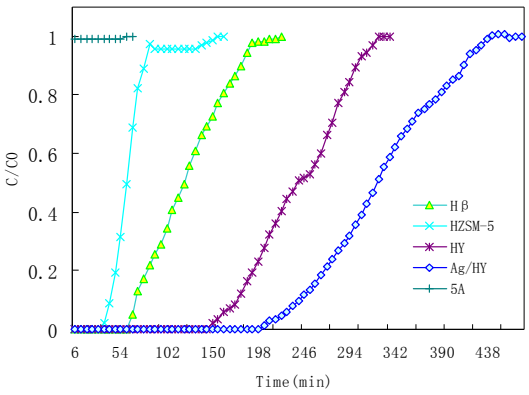

Fig. 2 The breakthrough curves of toluene on zeolites (samples: 200 mg, the inlet concentration of toluene: 100 ppm and flow rate: 300 ml/min)

In order to find out the relationship between structure and toluene adsorption, Ag/HY were characterized by XRD, XPS and SEM (Fig.3). Fig.3a showed that Ag/HY catalyst exhibited the typical peaks of HY, indicating that the structure of the zeolite did not changed during silver loading. Moreover, from the result of SEM analysis (Fig.3b), it could be noted that some Ag granules appeared and well dispersed on the surface of zeolite HY In addition, the Ag 3d photoelectron spectra (Fig.3c) indicated that the Ag species on the surface of catalyst was Ag^0, because the $Ag3d^{5/2}$ peak at 368.6 eV was assigned to metallic silver[24]. As shown in Fig.3b the particle size of metallic silver granules on the surface of Ag/HY was about 20nm. It has been proposed that metallic silver nanoparticles could work as adsorption centers for VOCs adsorption[25], and improve the chemical adsorption ability[26]. Moreover, Baek suggested that the metals which possessed empty s-orbits and available electrons in the d-orbits could form strong π-complexation bonding[23], and the π-complexation adsorption with toluene on Ag also contributed to the enhancement of adsorption abilities of Ag/HY catalyst. In addition, silver particles could entered into the particular pore channels of support, resulting in the formation of new pore tunnel and new surface area for toluene adsorption[25].As a result, the Ag/HY owned better toluene adsorption than zeolite HY.

3.2. Catalytic activity evaluation

Fig.4 showed a typical result of toluene removal using the NTP reactor with a representative sample (zeolite Hβ). At the first stage (Stage I), toluene was adsorbed on Hβ. The Hβ was broke through at 42 min and it reached saturation at 192 min. Then, the plasma was turned on (Stage Ⅱ). During this stage, concentration of CO and CO_2 immediately increased and then quickly decreased, and finally remained at a steady value. The concentration of toluene also showed the same tendency, which indicated that toluene desorbed firstly and then a new adsorption-desorption equilibrium appeared under discharge condition. At the third stage (StageⅢ), plasma was off again, and the CO and CO_2 vanished immediately, whereas the concentration of toluene slowly recovered to influent concentration, which meant that adsorption of toluene occurred. Compared to the adsorption stages (Stage Ⅰ), adsorption capacity of toluene at Stage Ⅲ showed no significant variation.

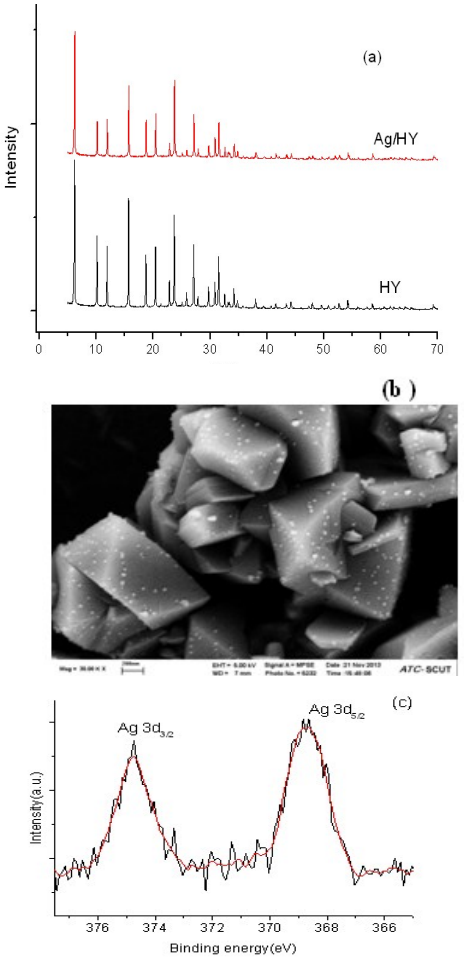

Fig. 3 XRD patterns (a), SEM image (b) and XPS(c) of Ag/HY catalyst

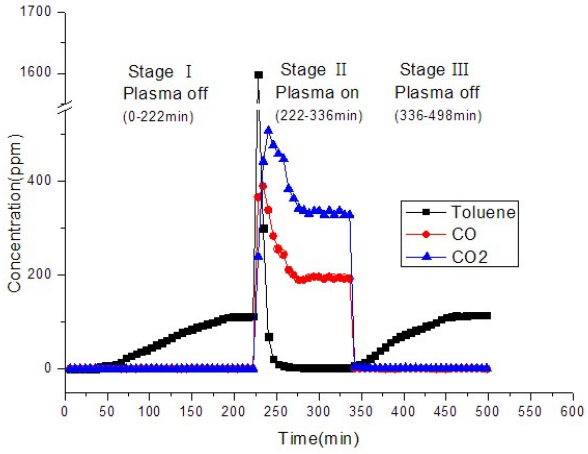

Fig. 4 Typical run of toluene removal in the catalysts combined NTP process (Catalyst: zeolite Hβ, toluene inlet concentration:110 ppm, input discharge power: 3.5 W and catalyst amount:200 mg.)

Catalytic activity of zeolites was determined at the stable states of the discharge reaction (Stage Ⅱ). Fig.5 showed the toluene removal efficiency (TRE), carbon balance and CO_2 selectivity during this period. The result revealed that whatever type of zeolite was introduced into the discharge zone, its toluene removal efficiency was significantly higher than the plasma system without zeolite, and the synergy of NTP and zeolite enhanced the toluene removal efficiency with an increment of approximately 37-56%. Previous researches reported that natural coulombic electric field in the microporous structure of zeolites could strengthen the discharge effect and enhance toluene conversion[27, 28]. Moreover, in the plasma combined catalysis system, the effect of ozone, adsorption/desorption and the direct interaction of gas phase radicals with catalyst surface was also related to toluene removal [10, 11,29].

In addition, the toluene removal efficiencies of NTP with different zeolites were different. Fig.5 exhibited that the toluene removal efficiencies in the combined system with zeolites 5A,HZSM-5,HY and Hβ were 79.8%, 80.8% 85.2% and 98.4%, respectively. Specifically, zeolite 5A did not adsorb toluene, but it exhibited high toluene removal efficiency. This may be attributed to strong collision of electrons and radicals in micropore, resulting in high discharge effect in unit volume [6] and more toluene molecular impacted by energetic electrons in the gas. Since other zeolites all had significant toluene adsorption capacity, their toluene conversion ability might depend on both electron impact in the gas phase and adsorption on the surface of zeolite. Furthermore,Fig.5. also showed the similar increment in toluene removal efficiency with different zeolites (5A, HZSM-5 and HY),which suggested that the toluene adsorption ability of these zeolites had an insignificant effect on the increase of toluene removal efficiency.

However, toluene adsorption ability greatly influenced the carbon balance and CO_2 selectivity. The carbon balance and CO_2 selectivity followed the order of HY>Hβ (HZSM-5)>5A, which was in agreement with toluene adsorption ability (Fig.2), indicating that the better performance of toluene adsorption, the more complete oxidation of toluene. Moreover, the oxidation improvement was positively proportional to the porosity of the catalysts[30]. Compared to zeolites 5A, Hβ and HZSM-5, zeolite HY owned biggest pore diameter that allowed more toluene to transport into the internal pore and provided largest surface area for toluene adsorption. It was well known that the surface of a catalyst can be activated by the plasma and then adsorb active species[31]. These active species could ultimately promote the toluene oxidation. Thus, highest toluene mineralization was achieved in the reactor with zeolite HY as catalyst.

In order to further promote the performance of the combined system, Ag was loaded on the surface of zeolite HY and toluene removal efficiency, carbon balance and CO_2 selectivity increased from 85.2%, 83.0% and 69.0% to 97.0%, 98.1% and 93.3%, respectively (Fig.3). For the reason, one side, Ag/HY showed better toluene adsorption ability than zeolite HY (Fig.2), and according to the analysis above, more adsorbed toluene was completely oxidized. The other side, the enhancement of mineralization will be confirmed by the decrease of byproducts in the section 3.4.

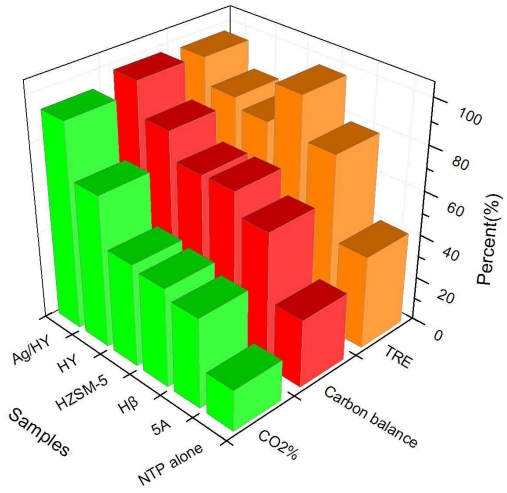

Fig. 5 TRE, carbon balance and CO_2 selectivity in plasma catalytic of toluene (The air flow rate: 300 ml/min, toluene initial concentration: 100 ppm, and input discharge power: 3.5 W.)

3.3 Byproducts

3.3.1 Ozone

Ozone is one of the major byproducts for oxygen-containing waste gas treatment in the DBD plasma. In this work, the ozone yield was observed to increase in the system with all zeolites (Fig.6) which was consistent with the findings by Chen Lin [32]. The reason might be explained that the discharge effect was strengthened by the catalyst packed in the discharge zone, which was verified by emission spectra analysis[32]. As a result, more ozone formed than that of the NTP alone system. However, the result was contrary to most current researches[33-39], which verified that the yield of ozone greatly

decreased by the addition of catalysts in the plasma system. Relevant experimental system about ozone decreased can be summarized into two cases. In the first, catalysts including $La_{0.8}Sr_{0.2}MnO_3/Al_2O_3$/Al-wire mesh[33] and $MnOx/Al_2O_3$/nickle foam[34,35] were coated onto the electrode but not packed in the discharge zone, and there was less surface discharge in the reaction space of NTP. In the second, catalyst $MnOx/Al_2O_3$ [36-39]was packed downstream after the plasma zone, i.e. post plasma catalysis system, and the catalysts could not influence the plasma discharge. In both cases, ozone can be decomposed by catalytic reaction, resulting in ozone formation decrease. Therefore the variation of ozone production in the plasma-catalysis system may be relevant to the way of catalysts being introduced into the system.

The decomposition of ozone in the plasma-catalysis system can be expressed as the following reactions[40]:

$$O_3 + Z \rightarrow Z-O_3 \qquad (R_1)$$
$$Z-O_3 \rightarrow Z-O^* + O_2 \qquad (R_2)$$

Here, Z-O_3 refers to ozone adsorbed on zeolite surface, Z-O* represents for atomic oxygen. R_1 and R_2 revealed that ozone was adsorbed on the surface of the catalyst and subsequently dissociated into atomic oxygen specie, which was found to be effective for toluene oxidation[41]. Hence, the ozone adsorption ability of zeolites may obviously affect ozone yield. In this work, as shown in Fig.6 the production of ozone was in the order of 5A>Hβ>HZSM-5>HY>Ag/HY. Ozone (5.8Å) and toluene (5.85Å) were inaccessible to the pore of the zeolite 5A [20].Therefore there was no adsorption and sequent dissociation of ozone on the surface of zeolite A, leading to high concentration of ozone exhaust. However, ozone could be accessible to the pore of other zeolites and then dissociated to atomic oxygen species which would react with toluene, resulting in ozone decreased. Moreover, it could be found that ozone yield in zeolite Ag/HY system was even lower than the value of NTP alone system. It seemed that besides those ozone adsorbed on the surface of zeolite, the surface of metallic Ag can also uptake ozone and form active oxygen on the surface[42], causing the further decrease of ozone yield.

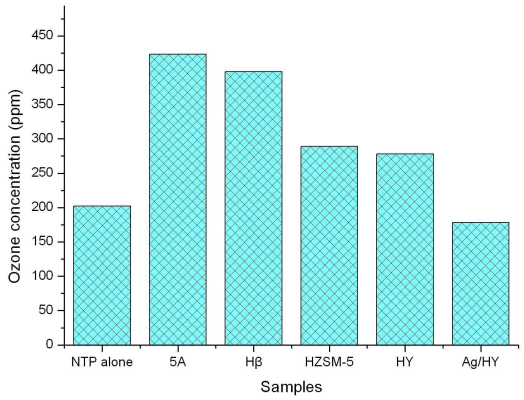

Fig. 6. The ozone yield with zeolite combined non thermal plasma reaction (Initial flow rate: 300 ml/min, toluene inlet concentration: 100 ppm, and input discharge power : 3.5 W.)

3.3.2 Organic byproducts on the surface of zeolite catalysts

Fig.7 showed the organic byproducts of toluene destruction in the zeolites combined NTP process. The detected byproducts were listed in Table 2. Eleven kinds of organic byproducts from toluene destruction by the plasma reaction combined with zeolites were identified. Among these byproducts, benzene, benzaldehyde, benzyl alcohol, phenol and o-xylene were ring-retaining products. According to the previous research[35], these ring-opening byproducts were also identified in the gas-phase during the toluene destruction by the NTP processes. That meant zeolites could trap gas-phase organic byproducts during DBD discharge. Other products (ethane,heptane, dodecane, hexadecane,pentadecane and heneicosane) also indicated that aromatic ring had been opened during toluene destruction by plasma combined zeolite. Van Durme gave both ring-retaining and ring-opening products of toluene degradation by positive corona discharge, and the ring-opening byproducts were not agreed with this study[43]. The reason may be ascribed to the difference of discharge way.

Compared to the relative abundance of byproducts on the surface of various zeolites, it could be found that there were much fewer productions on the surface of zeolite 5A than on that of other zeolites. This phenomenon was similar with the research of Tao Jiang et al.[28], who conducted the investigation on methane conversion using zeolite A combined with dielectric-barrier discharge and drew a conclusion that zeolite A inhibited the formation of carbon black and plasma polymerized film[28]. In addition, zeolite 5A could not adsorb molecules bigger than its pore size in the gas-phase, and only a small

amount of deposition of the aerosol byproducts on the external surface. However, zeolites HY, Hβ and HZSM-5 owned excellent toluene adsorption ability and enhanced the conversion of toluene, resulting in more byproducts. Meanwhile, they can serve as reservoirs for gas-phase organic compounds and deposited aerosol due to their particular pore structure and surface characteristics. Therefore, there were more materials appeared on their surfaces than that on the surface zeolite 5A. Furthermore, majority of detected byproducts in bare zeolites reaction were not found when Ag/HY catalysis was combined with NTP reaction in this study, because the metallic silver can decompose ozone and form active oxygen which was beneficial to deep oxidation of the reaction intermediates[42].

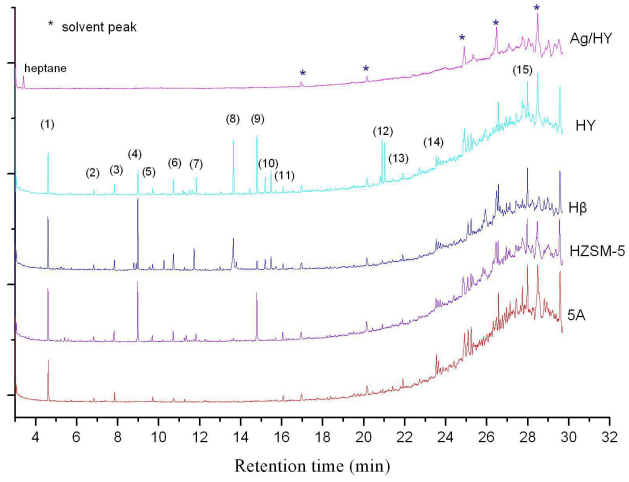

Fig. 7 GC-MS chromatogram of organic byproducts on the surface of zeolites

Table 2 organic byproducts of toluene decomposition on the surface of zeolites

Peak number	Retention time(min)	Byproducts
(1)	4.601	Toluene
(2)	6.760	O-xylene
(3)	7.834	Ethane
(4)	8.981	Benzaldehyde
(5)	9.699	Heptane
(6)	10.714	Benzyl Alcohol
(7)	11.828	Benzaldehyde
(8)	13.642	Benzene
(9)	14.792	Benzene
(10)	15.191	Phenol
(11)	16.056	Dodecane
(12)	21.019	Benzene
(13)	21.950	Hexadecane
(14)	23.633	Pentadecane
(15)	27.979	Heneicosane

3.4 Mechanism of toluene decomposition in plasma-catalysis system

The possible pathways of toluene decomposition by NTP combined catalysis were showed in Fig.8, which based on the suggestion that toluene could be destructed mainly by electron impact and active species (e.g.O_3, O and OH) oxidation[35]. Generally, the pathway of toluene destruction was closely related to the bond energy of chemical groups. In this work, the average energy of electron in NTP is up to 10 eV[44], and the bond energy of C-H in the methyl group is the smallest one (3.7 eV) compared to other bonds including C-H in aromatic ring (4.3e V),C-C between methyl group and aromatic ring (4.4 eV), C-C in aromatic ring (5.0-5.3 eV) and C=C in aromatic ring(5.5 eV)[45]. Therefore, the primary process of toluene oxidation was the breaks of C-H in methyl group. C-H in methyl group could be damaged by high energy electron and abstracted by hydroxyl radical in non thermal plasma[43], resulting in formation of a benzyl radical. Then the benzyl radical could react with oxygen species and formed benzaldehyde and benzyl alcohol. In addition, C-C between methyl group and benzene ring could be broke to form phenyl group, which can bond with H·, OH· and CH_3· to produce benzene, phenol and o-xylene, respectively. And the ring-containing intermediate products could be further opened by energetic electron to produce ring-opening intermediates[35]. Furthermore, in plasma system, cracking and polymerization reactions could occur simultaneously. As a result, ring-opening intermediates could crack or polymerize to form ethane, heptane, dodecane, hexadecane, pentadecane and heneicosane. Huang H.B. proposed the reaction pathways of toluene decomposition in NTP-catalysis system and only ring-retaining products were detected in the proposed pathways, but the step of ring-opening was pointed out and ring-opening intermediates were finally oxidized to CO_2 and H_2O[35].

Journal Name RSCPublishing

ARTICLE

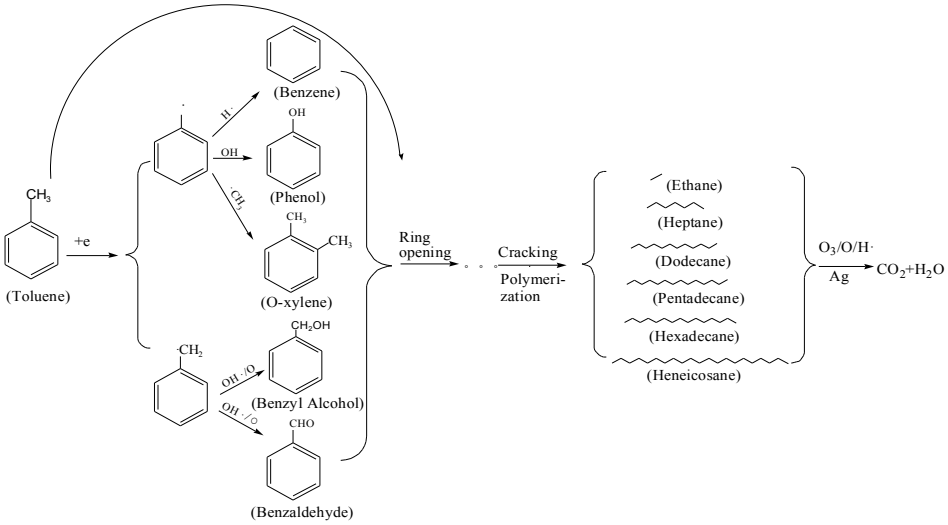

Fig. 8 The pathways of toluene decomposition by plasma –catalysis system

In plasma-catalysis system, homogenous reaction in the gas-phase and heterogeneous reaction on the solid surface of catalysts were considered to be two main reactions for pollutants decomposition. Fig.4 showed that there were both adsorption and desorption of toluene occur on the surfaces of zeolites during discharge process. So in the process of plasma-catalytic oxidation of toluene, homogeneous and heterogeneous reaction took place together. In the gas phase, toluene destruction mainly depended on the attack of energetic electrons. However, on the interface of gas phase and solid zeolite surface, the process of toluene decomposition was complicated. Compared to the reaction of toluene with atomic oxygen (5.7×10^{-12}cm^3 mol^{-1} s^{-1}) ,the reaction of ozone with toluene in the gas-phase is very slow (1.2×10^{-20} cm^3 mol^{-1} s^{-1})[36], and plasma-generated ozone alone can not destroy pollutants completely. Therefore, it could be inferred that it was primarily the atomic oxygen species that oxidize toluene. Besides that, from the results of Fig.2, Fig.5 and Fig.6, the carbon balance and CO_2 selectivity followed the order of HY > Hβ (HZSM-5)>5A which was agreement with toluene adsorption abilities, while opposed with the ozone emission. Therefore, adsorption ability of toluene and ozone play important roles, and it was the adsorbed toluene that reacted with atomic oxygen, which was responsible for the complete oxidation of toluene.

According to the adsorption features of various types of zeolites, toluene decomposition on zeolites could be described as following reactions (R_3 to R_8)[10, 46]:

$$C_7H_8(g)+e \rightarrow CO+CO_2+IM \quad (R_3)$$
$$C_7H_8(g)+Z \rightarrow Z-C_7H_8* \quad (R_4)$$
$$Z-C_7H_8*+Z-O* \rightarrow CO+CO_2+IM \quad (R_5)$$
$$Ag+O_3 \rightarrow Ag-O*+O_2 \quad (R_6)$$
$$IM+Ag-O* \rightarrow CO+CO_2 \quad (R_7)$$
$$CO+Ag-O* \rightarrow CO_2 \quad (R_8)$$

Here, Z and IM are behave of zeolites and intermediates, respectively, Z-O_3 refers to ozone adsorbed on zeolite surface, and Z-O* represents for atomic oxygen. Zeolite 5A showed excellent toluene removal efficiency, high ozone emission and low CO_2 selectivity. This results indicated that energetic electron impact toluene molecules in gas reaction ($C_7H_8(g)$) was one of the reactions of toluene decomposition (R_3) since zeolite 5A was considered lacking the ability of toluene and ozone adsorption. In contrast, for other zeolites which possessed adsorption abilities of both toluene and ozone, carbon balance and CO_2 selectivity were enhanced and ozone was further decreased with these types of zeolites. This demonstrated that adsorbed toluene ($Z-C_7H_8*$) were decomposed by oxygen atomic $Z-O*$ which dissociated by adsorbed ozone (R_4 and R_5). Moreover, Ag/HY exhibited better CO_2 selectivity than

HY, displaying an important role of Ag in the decomposition of the surface intermediates[42]. It also revealed that the intermediates (IM) in the reactions of R_3 and R_5 might be deposited or adsorbed on the surfaces of zeolites and further decomposed by Ag. So the heterogeneous reaction of NTP-catalyst oxidation of toluene followed Langmuir-Hinshelwood mechanism.

4. Conclusion

Zeolites with various sizes showed great effects on the toluene removal in non-thermal plasma reactor and several conclusions could be drew in this work. Firstly, all of the zeolites could improve the toluene removal efficiency, carbon balance and CO_2 selectivity of toluene oxidation. Secondly, toluene removal efficiency depended on discharge effect of NTP and toluene adsorption ability of catalysts, and toluene adsorption ability of catalysts was mainly responsible for the improvement of carbon balance and CO_2 selectivity. Lastly, loading silver can further decrease the organic byproducts and enhance mineralization of toluene oxidation.

Acknowledgements

The authors would like to acknowledge the financial support for this work by the National Natural Science Foundation of China. (No.50978103, No.U1201231), the National High-tech Research and Development Program of China（No.2013AA065005）and the fund of Guangdong Provincial Key Laboratory of Atmospheric Environment and Pollution Control of China.

Notes and references

a College of Environment and Energy, South China University of Technology, Guangzhou 510006, P.R. China
b Guangdong Provincial Key Laboratory of Atmospheric Environment and Pollution Control of China, Guangzhou 510006, P.R. China
c South China Agricultural University, Guangzhou, 510642, P.R. China

1. J. Ma, X. Xu, C. Zhao and P. Yan, *Adv. Atmos. Sci.*, 2012, **29**, 1006-1026.
2. W. B. Li, J. X. Wang and H. Gong, *Catal. Today*, 2009, **148**, 81-87.
3. G. Xiao, W. Xu, R. Wu, M. Ni, C. Du, X. Gao, Z. Luo and K. Cen, *Plasma Chem. Plasma Process.*, 2014, **34**, 1033-1065.
4. Faisal I. Khan , Aloke Kr.Ghoshal, *J Loss. Prevent. Proc.*, 2000,13,527–545
5. H.-H. Kim, *Plasma Process Polym.*, 2004, **1**, 91-110.
6. F. Holzer, F. D. Kopinke and U. Roland, *Plasma Chem. Plasma Process.*, 2005, **25**, 595-611.
7. G. Lombardi, N. Blin-Simiand, F. Jorand, L. Magne, S. Pasquiers, C. Postel and J. R. Vacher, *Plasma Chem. Plasma Process.*, 2007, **27**, 414-445.
8. J. Wu, Q. Xia, H. Wang and Z. Li, *Appl .Cata. B-Environ.*, 2014, **156–157**, 265-272.
9. Atsushi Ogata, Daisuke Ito, Koichi Mizuno, Satoshi Kushiyama, and Toshiaki Yamamoto, IEEE Trans.Ind.appl., 2001.37(4):959-964.
10. Q. H. Trinh, M. S. Gandhi and Y. S. Mok, *Jpn. J. of Appl. Phys.*, 2015, **54**, 01AG04.
11. M. Lu, R. Huang, J. Wu, M. Fu, L. Chen and D. Ye, *Catal. Today*, 2015, **242**, 274-286.
12. U. Roland, F. Holzer and F. D. Kopinke, *Appl. Catal. B- Environ.*, 2005, **58**, 217-226.
13. H.-H. Kim, Y. Teramoto, T. Sano, N. Negishi and A. Ogata, *Appl. Catal. B-Environ.*,2015, **166-167**, 9-17.
14. Chang-jun Liu, Jia-xin Wang, Kai-lu Yu ,Baldur Eliasson, Qing Xia, Bingzhang Xue, Yu-hang Zhang. J. Electrostat. 2002, 54 :149–158
15. S. M. Oh, H. H. Kim, H. Einaga, A. Ogata, S. Futamura and D. W. Park, Thin Solid Films, 2006, 506-507, 418-422.
16. Tomoyuki Kuroki,Kiyoyuki Hirai, Shigeru Matsuoka,Jong Youl Kim, and Masaaki Okubo, IEEE Trans. Ind. Appl., 2011, 47,1916-1921
17. Tomoyuki Kuroki, Kiyoyuki Hirai, Ryouhei Kawabata, Masaaki Okubo and Toshiaki Yamamoto, IEEE Trans. Ind. Appl 2010,46,672-679
18. Baldur Eliasson, Chang-jun Liu, and Ulrich Kogelschatz, Ind. Eng. Chem. Res. 2000, 39, 1221-1227.
19. Kui Zhang, Baldur Eliasson, and Ulrich Kogelschatz, Ind. Eng. Chem. Res. 2002, 41, 1462-1468
20. C. Y. Chao, C. W. Kwong and K. S. Hui, *J. Hazard. Mater.*, 2007, **143**, 118-127.
21. C. Wen, A. Yin and W.-L. Dai, *Appl. Catal. B- Environ.*, 2014, **160-161**, 730-741.
22. J.-H. Park, S. J. Park, I.-S. Nam, G. K. Yeo, J. K. Kil and Y. K. Youn, *Micropor. Mesopor. Mater.*, 2007, **101**, 264-270.
23. S.-W. Baek, J.-R. Kim and S.-K. Ihm, *Catal. Today*, 2004, **93-95**, 575-581.
24. D.-Z. Zhao, X.-S. Li, C. Shi, H.-Y. Fan and A.-M. Zhu, *Chem. Eng. Sci.*, 2011, **66**, 3922-3929.
25. D. Chen, Z. Qu, S. Shen, X. Li, Y. Shi, Y. Wang, Q. Fu and J. Wu, *Catal. Today*, 2011, **175**, 338-345.
26. D. Chen, Z. Qu, Y. Lv, X. Lu, W. Chen and X. Gao, *J. Mol. Catal. A-Chem.*, 2015, **404-405**, 98-105.
27. Brama Raju,Elinga Reddy,J Karupplah,Pmanoj Kumar Reddy and Ch Subrahmanyam, J. Chem. Sci.2013,125,673–67..
28. Tao Jiang,Yang Li, Chang-jun Liu，et al Catal. Today. 2002, 72,229–235.
29. H.-H. Kim, A. Ogata and S. Futamura, *App. Catal. B- Environ.*, 2008, **79**, 356-367.

30. U. Roland, F. Holzer, F.-D. Kopinke,Catal. Today, 2002, 73,315–323

31. H.-H. Kim, Y.-H. Lee, A. Ogata and S. Futamura, *Catal. Commun.*, 2003, **4**, 347-351.
32. L. Chen, X. Zhang, L. Huang and L. Lei, *J. Nat. Gas Chem.*, 2010, **19**, 628-637.
33. Y. Sun, L. Zhou, L. Zhang and H. Sui, *J. Environ. Sci.*, 2012, **24**, 891-896.
34. Y. Guo, X. Liao, J. He, W. Ou and D. Ye, *Catal. Today*, 2010, **153**, 176-183.
35. H. Huang, D. Ye, D. Y. C. Leung, F. Feng and X. Guan, *J. Mol. Catal. A-Chem.*, 2011, **336**, 87-93.
36. A. M. Harling, D. J. Glover, J. C. Whitehead and K. Zhang, *Appl. Catal. B- Environ*. 2009, **90**, 157-161.
37. X. Fan, T. L. Zhu, M. Y. Wang and X. M. Li, *Chemosphere*, 2009, **75**, 1301-1306.
38. J. Jarrige and P. Vervisch, *Appl. Catal. B- Environ*. 2009, **90**, 74-82.
39. T. Zhu, J. Li, W. Liang and Y. Jin, *J. Hazard. Mat.*, 2009, **165**, 1258-1260.
40. M. Magureanu, N. B. Mandache, P. Eloy, E. M. Gaigneaux and V. I. Parvulescu, *Appl. Catal. B- Environ.*, 2005, **61**, 12-20.
41. S. Delagrange, L. Pinard and J. Tatibouet, *Appl. Catal. B- Environ.*, 2006, **68**, 92-98.
42. H.-H. Kim, M. Sugasawa, H. Hirata, Y. Teramoto, K. Kosuge, N. Negishi and A. Ogata, *Plasma Chem. Plasma Process.*, 2013, **33**, 1083-1098.
43. J. Van Durme, J. Dewulf, W. Sysmans, C. Leys and H. Van Langenhove, *Chemosphere*, 2007, **68**, 1821-1829.
44. Y.-F. Guo, D.-Q. Ye, K.-F. Chen, J.-C. He and W.-L. Chen, *J. Mol. Catal. A:-Chem.*, 2006, **245**, 93-100.
45. Hitoshi Kohno, Alexander A. Berezin, Jen-Shih Chang, Minoru Tamura,Toshiaki Yamamoto, Akira Shibuya, and Shigeo Honda, IEEE Trans. Ind. Appl., 1998,34,953-966

46.J. Li, H. Na, X. Zeng, T. Zhu and Z. Liu, Appl. Surf. Sci., 2014, 311, 690-696.

